LUDWIG-
MAXIMILIANS-
UNIVERSITÄT
MÜNCHEN

FAKULTÄT FÜR PHYSIK
UNIVERSITÄTSSTERNWARTE MÜNCHEN

MASTERPROGRAMM FÜR ASTROPHYSIK
BASICS ASTROPHYSICAL LAB





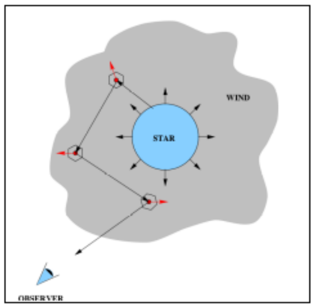

Weak gravitational lensing

The 2-point correlation function of cosmic shear

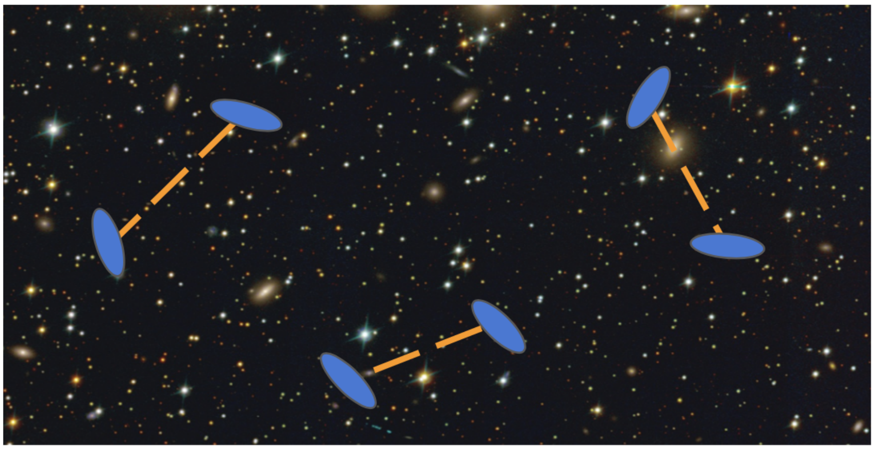

Authors: Zhengyangguang Gong[A,B], Anik Halder[A,B]

A: Responsible for the experimental design and the concept of the lab
B: Major Contributions to the Lab Manual
C: Minor Contributions to the Lab Manual

Panel images (page-top) courtesy of USM website - https://www.usm.uni-muenchen.de/

Cover image: The correlation between galaxy shapes after the coherent distortion of the weak gravitational lensing can be described by the cosmic shear 2-point correlation function (2PCF). The values of the 2PCF vary as the angular separation (size of the orange dashed lines) between the projected galaxy shapes (blue ellipses) change. Background image: Perseus galaxy cluster observed with the 2m Fraunhofer telescope at the Mt. Wendelstein Observatory of LMU Munich.

Preface

Important: Please read this first!

- **Read the lab manual very carefully already before the first day of the lab!** You are expected to spend substantial amount of time at home studying the lab manual.
- **Go through and perform the instructions provided** in the 'Software requirements for this lab' (see next page).
- **Theoretical exercises (T1-T6)** should ALREADY be attempted at home while preparing for the first day of the lab. They are very important for understanding the theoretical background of the lab. Note that students might be asked to present and discuss their solutions during the lab session and also include them in the lab report.
- **Experimental exercises** are intended to be done on the first **(P1.1-P1.6)** and second **(P2.1-P2.7)** days of the lab and their solutions should be included in the final lab report as well.
- Your final lab report has to contain the complete solutions to all exercises. For the theoretical problems you can either write them up in LaTeX or turn in (scanned version of) your handwritten solutions (they should be neat and legible) along with your lab report.

In general, the lab is written for `python` users. It is our wish that while working through this lab, students not only understand and grasp the main concepts of weak lensing cosmology but also get familiar with scientific programming in `python`. The latter is an essential and extremely valuable tool that will help students a lot during their master projects and further research endeavours. To this end, we highly encourage students to learn and develop their `python` programming skills through the exercises we have designed in this lab. An extremely valuable resource (which has helped both the authors of this lab to learn `python`) is this excellent week-long tutorial: https://astrofrog.github.io/py4sci/ .

The lab manual is not error free, so please do let your supervisors know in case you spot errors and typos! Any feedback during and after the lab will always be highly appreciated. We hope that you have fun doing the lab.

- Anik and Zhengyangguang

Software requirements for this lab

We will use `python` and `jupyter notebook` for this lab. You'll need the following packages:

- `numpy`, `scipy` and `matplotlib`. You can use `pip` or `conda` to install them.
- `CLASS` (https://github.com/lesgourg/class_public) - the package can be installed online from the github repository (for the latest version). An easier option which installs a slightly older version (but is sufficient for our lab) can be obtained with:
  `pip install classy`
- `healpy` (https://healpy.readthedocs.io/en/latest/install.html). You can install this with: `pip install --user healpy`
- `TreeCorr` (https://rmjarvis.github.io/TreeCorr/_build/html/overview.html). You can install this with: `pip install treecorr`

Please install these packages well in advance before the lab on either:

- Your own computer. Consult your supervisor already before the day of the lab if you have problems with the installation and need help.
- Or use your account on the `LMU physik jupyterhub` portal[1]! where they are *already installed* in the python environment `python/3.11-2023.09`. Simply start your cip pool session with this specific python environment.

To test whether the installation of the packages worked or not, open a `jupyter notebook` and in a cell execute the following code snippet:

```
import numpy as np
import scipy
import matplotlib.pyplot as plt
from classy import Class
import treecorr
import healpy as hp
```

If there are no errors, then your installation of these packages has been successful!

Once the packages are installed, **download the code and data which are needed for the lab exercises** from:
https://datashare.mpcdf.mpg.de/s/iQL4nUmrDaYzmfP . From the terminal you can simply perform:

```
wget https://datashare.mpcdf.mpg.de/s/iQL4nUmrDaYzmfP/download
unzip download
rm -rf download
```

[1] https://jupyter.physik.uni-muenchen.de/hub/login

1 Introduction

Weak gravitational lensing involves the study of the cosmic shear field — coherent distortions imprinted in the shapes of background source galaxies by the gravitational lensing effect of the foreground matter distribution in the Universe (Bartelmann & Schneider 2001; Schneider et al. 2006; Kilbinger 2015). Statistical analyses of cosmic shear data thus let us directly probe the large-scale structure in our Universe, and consequently, enable us to place tight constraints on the parameters of our cosmological models and address key questions such as the nature of dark energy, dark matter and gravity. Indeed, cosmic shear data has already had a marked impact in cosmology, most notably with the recent analyses of the data from large photometric galaxy surveys like the Dark Energy Survey (DES Collaboration 2021), Kilo Degree Survey (Heymans et al. 2021) and Hyper-Suprime Cam Survey (Hikage et al. 2019), and this progress is expected to be taken to a whole new level when the data from the larger Euclid (Laureijs et al. 2011), Vera Rubin (LSST Dark Energy Science Collaboration 2012) and Nancy Roman (Spergel et al. 2015) surveys are available in the future. The main statistical tool employed by all these surveys to analyse cosmic shear data are the so-called cosmic shear 2-point correlation functions $\xi_\pm$ (Troxel et al. 2018).

In this lab we will study the theory behind this widely popular 2-point shear statistic and how we can model it as a function of cosmological parameters. We will also measure this statistic in simulated cosmic shear data obtained from realistic N-body simulations of our Universe. The final goal of the lab would be to see whether our analytical calculations and our measurements of the shear 2-point correlation function are in agreement or not.

2 Basic concepts in cosmology

Before we step into the topics of weak gravitational lensing, it is necessary for us to briefly outline some basic cosmological concepts which should help you understand the content of the manual. Most of you should already be familiar with topics such as standard ΛCDM cosmological model, redshift and distance measurement after participating in relevant cosmological lectures. For more details, we recommend students to read Dodelson & Schmidt (2020), Peacock (2012) and Mukhanov (2005).

2.1 Standard cosmological model

We have concrete evidence to show that our Universe is expanding. To describe the increasing distance between two points in the Universe, it is convenient to introduce the scale factor $a(t)$. The contemporary value of it is set to one and it becomes smaller until zero when we trace back in time to the beginning of the Big Bang. The actual physical distance d between two points is then proportional to the multiplication of the scale factor and the comoving distance χ:

$$d = a(t)\chi \, , \tag{1}$$

where χ is defined in the *comoving coordinates*. This coordinate system expands uniformly along with the Universe and thus the comoving distance remains constant with respect to time.

In order to measure distances in the Universe, we also need to know its geometry. There are three possibilities which are parametrized by the spatial curvature k:

- Euclidean (Flat): The Euclidean space with $k = 0$ and the Universe is of infinite volume.
- Open: A hyperbolic universe which can be imagined locally as an infinitely extended saddle surface with $k < 0$.
- Closed: Analogous to the surface of a sphere with constant positive curvature $k > 0$.

With the above ingredients, we can write the differential 3D spatial distance in an expanding curved universe in a spherical coordinate system as:

$$\mathrm{d}l_{3d}^2 = a^2(t)\left(\frac{\mathrm{d}r^2}{1-kr^2} + r^2(\mathrm{d}\theta^2 + \sin^2\theta \mathrm{d}\phi^2)\right), \tag{2}$$

where r is the comoving distance along the radial direction, and θ, ϕ are the polar and azimuth angles respectively.

However, the gravitational interaction in cosmology is described by the theory of General Relativity and in relativistic theory the spatial distance is not an invariant quantity with respect to coordinate transformations. In order to compute such an invariant in cosmology, we have to upgrade equation (2) to a four-dimensional spacetime in which the differential interval is calculated as:

$$\mathrm{d}s^2 = g_{\mu\nu}\mathrm{d}x^\mu \mathrm{d}x^\nu \tag{3}$$

$$= -\mathrm{d}t^2 + a^2(t)\left(\frac{\mathrm{d}r^2}{1-kr^2} + r^2(\mathrm{d}\theta^2 + \sin^2\theta \mathrm{d}\phi^2)\right), \tag{4}$$

where we use natural units such that the speed of light $c = 1$. Indices μ and ν go from 0 to 3 with 0 indicating the time coordinate t and 1 to 3 representing the spatial coordinates. The metric tensor g in the four-dimensional spacetime is the well known Friedmann–Lemaître–Robertson–Walker (FLRW) metric expressed in spherical coordinates.

Another aspect of general relativity is that it relates the metric to the constituents of the Universe. This relation is contained in the Einstein field equations which can be neatly written down as a collection of tensor equations:

$$G_{\mu\nu} + \Lambda g_{\mu\nu} = 8\pi G T_{\mu\nu} \,. \tag{5}$$

The first term on the left hand side of the equation is the Einstein tensor defined as:

$$G_{\mu\nu} \equiv R_{\mu\nu} - \frac{1}{2} g_{\mu\nu} R \,, \tag{6}$$

where $R_{\mu\nu}$ is the Ricci tensor and can be computed from the metric tensor and its derivatives. The scalar R is the Ricci scalar and is the contraction of the Ricci tensor $R = g^{\mu\nu}R_{\mu\nu}$. Λ is the cosmological constant and under the ΛCDM cosmological parametrization it is proportional to the dark energy density in the Universe. G on the right hand side of the equation is the gravitational constant and T is the energy-momentum tensor which characterises the constituents of the Universe such as matter, radiation and so on.

Based on equation (5), one can derive multiple equations governing the evolution of the Universe. Detailed derivations can be found in the previously mentioned references and here we just show some important results for a homogeneous and isotropic expanding universe. When $\mu = \nu = 0$, the metric only considers the time-time component and equation (5) becomes

$$G_{00} + \Lambda g_{00} = 8\pi G T_{00} \ . \tag{7}$$

If we substitute the tensor entries on both sides of the equation with their corresponding expressions, we obtain the **first Friedmann equation**:

$$\left(\frac{\dot{a}}{a}\right)^2 = \frac{8\pi G\rho}{3} - \frac{k}{a^2} + \frac{\Lambda}{3} \ , \tag{8}$$

where $\dot{a}$ represents the derivative of the scale factor with respect to time and ρ is the energy density of the constituents of the Universe such as matter and radiation. Next when considering the spatial part of equation (5) with $\mu = \nu = i$ where $i = 1, 2, 3$, we obtain the same equation for each index:

$$G_{ii} + \Lambda g_{ii} = 8\pi G T_{ii} \ , \tag{9}$$

from which the **second Friedmann equation** can be derived:

$$\frac{\ddot{a}}{a} = -\frac{4\pi G}{3}(\rho + 3p) + \frac{\Lambda}{3} \ , \tag{10}$$

where $\ddot{a}$ is the acceleration of the scale factor and p is the pressure of the constituents of the Universe. It is related to the corresponding energy density through the **equation of state**:

$$p = w\rho \ , \tag{11}$$

where w is the coefficient and has different values for different constituents in the Universe. We have $w_{\mathrm{m}} = 0$ for non-relativistic matter (can be baryonic matter [b] or cold dark matter [cdm]), $w_{\mathrm{r}} = 1/3$ for radiation [r] and $w_\Lambda = -1$ for the cosmological constant [Λ].

It is very common in the cosmology literature to quote the density of a constituent of the Universe in dimensionless units called the **density parameter** Ω_i which for a given species $i =$ [b, cdm, r, Λ] is defined via

$$\Omega_i \equiv \frac{\rho_i}{\rho_c} \tag{12}$$

where $\rho_c = 3H^2/(8\pi G)$ is called the critical density. For a flat universe ($k = 0 \implies \Omega_k = 0$), the sum of the density parameters for all the components which constitute the Universe equals[2] 1 i.e.:

$$\sum_i \Omega_i = 1 \ . \tag{13}$$

If we combine equation (8) and equation (10) we can derive the equation describing the energy density evolution:

$$\dot{\rho} = -3\frac{\dot{a}}{a}(\rho + p) \ , \tag{14}$$

where one can replace the pressure with the equation of state and solve the differential equation to obtain the energy density $\rho(a)$ of a specific constituent as a function of the scale factor a.

[2] You can readily see this from the first Friedmann equation. Try to write the expressions for Ω_Λ and Ω_k.

2.2 Redshift and distance measurement

Besides the scale factor, there is another commonly used quantity for the expansion: the redshift z. It is related to the fact that the physical wavelength of light emitted from a distant object is stretched proportional to the scale factor as it propagates towards the observer. It is defined as:

$$1 + z \equiv \frac{\lambda_{\rm obs}}{\lambda_{\rm emit}} = \frac{a(t_0)}{a(t_{\rm emit})} = \frac{1}{a(t_{\rm emit})} , \tag{15}$$

where $\lambda_{\rm obs}$ is the observed wavelength, $\lambda_{\rm emit}$ is the emission wavelength. In conclusion, we can write:

$$1 + z = \frac{1}{a(t)} . \tag{16}$$

In this subsection, we introduce two types of distance: One is the *comoving distance* and the other is the *angular diameter distance*. For simplicity, we only consider the scenario when the Universe has a flat geometry ($k = 0$) which will be relevant to our theoretical modelling later. Expressions for distances in a universe with non-zero curvature can be looked up in the previously mentioned references.

Comoving distance

Imagine a light ray is emitted from a distant object at time t and reaches the observer at the current time t_0. It travels along the *null-geodesic* which means $\mathrm{d}s^2$ in equation (4) is always equal to zero. If we assume that the light travels along the radial direction and all angular changes are zero, we have $\mathrm{d}r = \mathrm{d}\chi$ in equation (4) and the comoving distance between the observer and the object is given by:

$$\chi(t) = \int_t^{t_0} \frac{\mathrm{d}t'}{a(t')} . \tag{17}$$

One can rewrite the above equation as an integration over the redshift z. But before that we need to introduce an important quantity defined to describe the expansion rate of the Universe called the **Hubble parameter**:

$$H \equiv \frac{\dot{a}}{a} , \tag{18}$$

and if we combine this definition with equation (16), we can rewrite equation (17) as:

$$\chi(t) = \int_{a(t)}^{1} \frac{\mathrm{d}a'}{\dot{a}(t')a(t')} = \int_{a(t)}^{1} \frac{\mathrm{d}a'}{H(a')a^2(t')} = \int_0^z \frac{\mathrm{d}z'}{H(z')} , \tag{19}$$

where we exploit the relation that the redshift is zero at the current value of the scale factor $a(t_0)$.

Angular diameter distance

In cosmological observations, if we know that the physical size of an extended object in the sky is l and it subtends an angle of θ which we observe, we can define another distance measurement called the angular diameter distance:

$$d_A \equiv \frac{l}{\theta} . \tag{20}$$

The comoving size of the extended object can be represented as l/a and the comoving distance from the observer to that object is exactly what we derive in equation (19). Therefore we can write the angular size of the object in terms of comoving length scales $\theta = (l/a)/\chi$ and once we substitute the angular size in equation (20) with this expression, the angular diameter distance becomes:

$$d_A = a\chi = \frac{\chi}{1+z}\,, \tag{21}$$

where it's again important to remember that this is the angular diameter distance expressed in a Euclidean space where $k = 0$.

2.3 ΛCDM model of cosmology

The Big Bang paradigm can be parametrized by the ΛCDM model, also called the standard model of cosmology. It is a model with six independent free parameters which can well explain the major results of the current cosmological observations:

- The origin and anisotropies of Cosmic Microwave Background (CMB).
- The distribution of galaxies at large scales.
- The abundance of light elements such as hydrogen and helium today.
- The current accelerating expansing of the Universe.

In short, ΛCDM model proposes a Euclidean universe dominated in its energy budget by the non-baryonic cold dark matter and dark energy, where the current large scale structure of the universe originated from initial perturbations generated by an inflationary epoch. To better understand this model, we have to know the constituents of cold dark matter (CDM) and dark energy (Λ) which are both beyond the Standard Model of particle physics. More details are beyond the scope of this manual and interested readers can refer to the literature cited at the beginning of this Section.

3 Statistical measures of a density field

Galaxy surveys are necessary and powerful tools in order to probe the large scale structure (LSS) in our Universe. Galaxy surveys can be multi-dimensional in space: One-dimensional pencil-beam surveys have a geometry which is much more extended along the line of sight than across the sky, requiring the determination of distances to many galaxies at high redshift (Munoz et al., 2010). Two-dimensional applications either reveal the distribution of galaxies in the sky without determining distance, or correspond to redshift surveys along a great circle in the sky like the equator (Gott et al., 2005). Nevertheless, the main application is in three-dimensions with both a survey of galaxy clustering in the sky and a classification of galaxies into multiple *tomographic* redshift bins like the Dark Energy Survey (DES) (Dark Energy Survey Collaboration et al., 2021).

The extraction of quantitative information from these surveys require unbiased and accurate statistical techniques. In this lab, we will focus on the most popular statistic called the power spectrum and its real space counterpart: 2-point correlation function (2PCF). This statistic is going to be implemented on a simulated weak gravitational lensing shear map (relevant details will be discussed in later sections). Therefore for the purpose of a general discussion, we will first present in this section our statistical measures of a general continuous density field $\rho(\vec{x})$.

3.1 Density perturbation field and its correlation function

The cosmological principle describes our Universe as homogeneous and isotropic. However this can only be held true at large length scales. Surveys like SDSS (Sloan Digital Sky Survey) have already revealed that our Universe is homogeneous and isotropic on relatively large scales (~ 100 Mpc). However, there are prominent inhomogeneities in the matter density field developed upon the homogeneous and isotropic background on small scales as the result of the gravitational evolution of the Universe.

The values of the matter density field $\rho(\vec{x})$ themselves cannot effectively display the perturbed feature in the late Universe. Therefore we define the *density perturbation field* which works better with our statistical measures:

$$\delta(\vec{x}) \equiv \frac{\rho(\vec{x}) - \langle\rho\rangle}{\langle\rho\rangle} , \tag{22}$$

where we exploit the homogeneous property of the statistics that leads to $\langle\rho(\vec{x})\rangle = \langle\rho\rangle$ and we have $\langle\delta(\vec{x})\rangle = \langle\delta\rangle = (\langle\rho\rangle - \langle\rho\rangle)/\langle\rho\rangle = 0$ follow immediately. This implies that the average of the density perturbation field is always zero and this quantity cannot reflect the inhomogeneities of our Universe. Thus it would be more reasonable to describe inhomogeneities with the variance of the density perturbation field, $\langle(\delta - \langle\delta\rangle)^2\rangle = \langle\delta^2\rangle$, rather than its average.

However, the variance $\langle\delta^2\rangle$ just indicates the strength of the inhomogeneity at a single location but does not take into account the spatial correlations of density perturbations between different points. Hence we need to introduce another statistic named *2-point correlation function* (2PCF) ξ to obtain further information:

$$\xi(\vec{r}) \equiv \langle\delta(\vec{x})\delta(\vec{x} + \vec{r})\rangle , \tag{23}$$

where $\vec{r}$ is the displacement vector between two points in space and the angle bracket indicates an average over the volume. It is positive when the density perturbations at two positions always have the same sign and negative if their signs are opposite. Essentially, it investigates how the perturbations of separate points in real space correlate to each other. We can observe that when $\vec{r} = \vec{0}$ (this is known as *zero lag*), the correlation function becomes the variance of the density perturbation field: $\xi(\vec{0}) = \langle\delta(\vec{x})\delta(\vec{x})\rangle = \langle\delta^2\rangle$. From the homogeneous property, statistics like the 2PCF no longer depend on the positions of the two points but only on the separation between them. Moreover, statistical isotropy implies that its values are independent of the direction of the displacement vector between the two points and only depends on the length of that separation vector. Therefore, the 2PCF is a spherically symmetric quantity in three-dimensional space and can be simplified as $\xi(\vec{r}) = \xi(r)$.

similar to the three-dimensional correlation function $\xi(\vec{r})$, we can also write the angular 2-point correlation function in two-dimensional space. In this case only angular positions of points within the 3D density perturbation fields are known but not the distances to them. Therefore, when correlating perturbations of two field points on the 2D sky we have:

$$w(\hat{r}_1, \hat{r}_2) = \langle\delta^{2D}(\hat{r}_1)\delta^{2D}(\hat{r}_2)\rangle , \tag{24}$$

where $\hat{r}_1$ and $\hat{r}_1$ are unit vectors indicating directions (or angular positions). If the angular separation between the two points in the sky is $\vec{\theta}$, in analogy to the definition of correlation function and based on statistical homogeneity and isotropy discussed in the previous section, it can be written as:

$$w(\hat{r}_1, \hat{r}_2) = \langle\delta^{2D}(\hat{r}_1)\delta^{2D}(\hat{r}_1 + \vec{\theta})\rangle = w(\vec{\theta}) = w(\theta) , \tag{25}$$

which depends only on the separation angle between $\hat{r}_1$ and $\hat{r}_2$. Usually, when the flat-sky approximation is satisfied where the physical extension corresponding to the angular scale one wants to probe on the celestial sphere is much smaller than the line-of-sight distance to the targets, the angular separation θ can be expressed as a 2D vector in a flat sky plane.

3.2 Power spectrum of a density perturbation field

We suggest students to revise their knowledge about Fourier analysis before studying this section of the manual and solving the associated exercises. Students can refer to Arfken & Weber (2012) and familiarise themselves with the concepts of Fourier transform, the orthogonality and completeness of Fourier coefficients and convolution theorem. Here we just show the Fourier transform convention we adopt in this lab to describe a random continuous spatial density field ρ:

$$\rho(\vec{x}) = \frac{V}{(2\pi)^3}\int \rho(\vec{k})e^{i\vec{k}\cdot\vec{x}}\mathrm{d}\vec{k}\,, \tag{26}$$

and its inverse Fourier transform:

$$\rho(\vec{k}) = \frac{1}{V}\int \rho(\vec{x})e^{-i\vec{k}\cdot\vec{x}}\mathrm{d}\vec{x}\,, \tag{27}$$

where we take for granted that the above Fourier relations are in three-dimensional space and V is the survey volume in which observations are carried out. The $\vec{k}$ in the above equations are wave vectors and they are the Fourier space counterparts of the spatial coordinates in real space. One useful property of $\rho(\vec{k})$ when $\rho(\vec{x})$ is a real-valued field is[3]:

$$\rho(\vec{k}) = \rho^*(-\vec{k})\,, \tag{28}$$

where the $*$ sign denotes for complex conjugate.

3.2.1 Power spectrum

Now, in order to find the equation for the power spectrum, we will first need to reformulate the correlation function defined in equation (23). The two correlated density perturbation field points can be represented by their corresponding Fourier transform and we would have:

$$\begin{aligned}
\xi(\vec{r}) &= \langle \delta(\vec{x})\delta(\vec{x}+\vec{r})\rangle & (29)\\
&= \frac{V^2}{(2\pi)^6}\left\langle \int_k \delta(\vec{k})e^{i\vec{k}\cdot\vec{x}}\mathrm{d}\vec{k}\int_{k'}\delta(\vec{k}')e^{i\vec{k}'\cdot(\vec{x}+\vec{r})}\mathrm{d}\vec{k}'\right\rangle & (30)\\
&= \frac{V}{(2\pi)^3}\int_k |\delta(\vec{k})|^2 e^{i\vec{k}\cdot\vec{r}}\mathrm{d}\vec{k}\,. & (31)
\end{aligned}$$

The power spectrum is either defined as:

$$P(\vec{k}) \equiv \langle |\delta(\vec{k})|^2\rangle\,, \tag{32}$$

or alternatively as:

$$\langle \delta^*(\vec{k})\delta(\vec{k}')\rangle \equiv (2\pi)^3\delta_D(\vec{k}'-\vec{k})P(\vec{k})\,, \tag{33}$$

[3]It's a nice little exercise for you to prove this.

where δ_D is the 3-dimensional Dirac delta function. Then equation (31) can be written as:

$$\xi(\vec{r}) = \frac{V}{(2\pi)^3} \int_k P(k) e^{i\vec{k}\cdot\vec{r}} \mathrm{d}\vec{k} \,, \tag{34}$$

from which we see that correlation function is simply the Fourier transform of the power spectrum.

Exercise:
• **T1**: Complete the derivation from equation (30) to equation (31). During the process you may need to implement the Fourier analysis mentioned at the beginning of section 3.2.

3.2.2 Angular power spectrum

Instead of $\vec{r}$, one would generally use angular separation vector $\vec{\theta}$ as the displacement vector for correlation functions in real observations performed on the 2D celestial sphere. The Fourier counterpart of the angular separation vector is the multipole number vector $\vec{\ell}$ whose modulus only takes integers as we expand a density perturbation field on a spherical surface in terms of spherical harmonics[4].

The expansion of the density perturbation field at a given direction in spherical harmonics is:

$$\delta^{2D}(\hat{r}) = \sum_{\ell\geq 0} \sum_{m=-\ell}^{\ell} a_{\ell m} Y_{\ell m}(\hat{r}) \,, \tag{35}$$

where $\hat{r}$ is the unit vector pointing to a specific direction in the sky. $Y_{\ell m}$ are spherical harmonics and like the set of continuous wave vectors $\{e^{i\vec{k}\cdot\vec{x}}\}$ that appear in Fourier transform, they also form an orthogonal and complete set on the spherical sky. $a_{\ell m}$ are coefficients of spherical harmonics. ℓ is the multipole number and m is another index associated with different orientations of the vector $\vec{\ell}$.

One important mathematical property of spherical harmonics $Y_{\ell m}$ is:

$$\sum_m Y^*_{\ell m}(\hat{r}_1) Y_{\ell m}(\hat{r}_2) = \frac{2\ell+1}{4\pi} L_\ell(\cos\theta) \,, \tag{36}$$

where $\hat{r}_1$, $\hat{r}_2$ are two different unit pointing vectors, $\hat{r}_1 \cdot \hat{r}_2 = \cos\theta$ and $L_\ell(\cos\theta)$ is the Legendre polynomial of order ℓ. Analogous to the definition of power spectrum in equation (33), the angular power spectrum is defined as:

$$\langle a^*_{\ell m} a_{\ell' m'} \rangle \equiv \delta_{\ell\ell'} \delta_{mm'} C_\ell \,, \tag{37}$$

where $\delta_{\ell\ell'}$ and $\delta_{mm'}$ are Kronecker delta functions. Similarly, the corresponding definition to equation (32) for the angular power spectrum is

$$C_\ell = \langle |a_{\ell m}|^2 \rangle. \tag{38}$$

[4] Remember from your Quantum mechanics lecture how for a spherically symmetric system (e.g. Hydrogen atom) where the angular momentum is conserved, the solutions to the angular part of the Schrödinger equation are the spherical harmonics $Y_{\ell m}$.

Based on the definition of angular correlation function in equation (25), we can derive the relation between angular correlation function and angular power spectrum in a similar approach as that implemented for the three-dimensional correlation function and power spectrum:

$$w(\theta) = \langle \delta^{2D}(\hat{r}_1)\delta^{2D}(\hat{r}_2)\rangle \tag{39}$$

$$= \sum_{\ell m}\sum_{\ell' m'} \langle a^*_{\ell m} a_{\ell' m'}\rangle Y^*_{\ell m}(\hat{r}_1) Y_{\ell' m'}(\hat{r}_2) \tag{40}$$

$$= \frac{1}{4\pi}\sum_{\ell}(2\ell+1)C_\ell L_\ell(\cos\theta)\,, \tag{41}$$

Exercise:

• **T2**: Apply the mathematical properties presented in subsection 3.2.2 and try to complete the derivation from equation (39) to equation (40).

3.2.3 The projection of three-dimensional power spectrum

In order to successfully join the two pieces of information in two-dimensional and three-dimensional space described separately before, we are going to introduce the mathematics of projecting 3-dimensional power spectrum of density perturbation fields into 2-dimensional power spectrum within the flat-sky approximation and then apply the spherical correction which leads to the angular power spectrum.

The 2D density perturbation field towards direction $\hat{r}$ is given by a weighted line-of-sight projection along the comoving radial direction of the 3D density perturbation field:

$$\delta^{2D}(\hat{r}) = \int \mathrm{d}\chi\, q(\chi)\, \delta(\chi\hat{r}, \chi)\,, \tag{42}$$

where $q(\chi)$ is a kernel which weighs the 3D density perturbation at distance χ along the line of sight.

Starting from the equation above can show that the two-dimensional power spectrum P^{2D} itself can be written as a line-of-sight projection of the three-dimensional power spectrum $P^{3D} \equiv P$ (introduced in equation (32)), by applying the *Limber's approximation* (Limber, 1954):

$$P^{2D}(\vec{\ell}) = \int \mathrm{d}\chi\, \frac{q^2(\chi)}{\chi^2}\, P^{3D}\left(|\vec{k}| = \frac{|\vec{\ell}|}{\chi}, \chi\right). \tag{43}$$

The explicit expression for the weighting kernel $q(\chi)$ in the context of gravitational lensing will be introduced in a later section. $\vec{k}$ is the Fourier mode in three-dimensional space and again from statistical isotropy we have $P^{2D}(\vec{l}) = P^{2D}(l)$. The detailed derivation of the above equation (43) from equation (42) can be found in the appendix of Kaiser, 1992.

This two-dimensional power spectrum from the flat-sky and Limber's approximation generally agrees quite well with current observations such as the Dark Energy Survey and the Kilo Degree Survey. However, for the weak lensing cosmic shear field that we will investigate in our lab, a further correction is possible to partly correct this two-dimensional power spectrum under the flat-sky approximation to the corresponding one on the spherical sky, i.e. the angular power spectrum C_ℓ:

$$C_\ell(\ell) = \frac{(\ell+2)(\ell+1)\ell(\ell-1)}{(\ell+0.5)^4} P^{2D}\left(\ell + \frac{1}{2}\right). \tag{44}$$

From equation (44), also called the *Kitching correction* (Kitching et al. 2017), one can easily calculate the angular correlation function using equation (41). In principle, the summation of ℓ should go up to infinity. However, since generally the angular power spectrum asymptotically approaches zero at large ℓ, we can stop the summation at a sufficiently large ℓ and obtain a fairly accurate result for the correlation function.

4 Basic theory of weak gravitational lensing

As predicted by the theory of General Relativity, light coming to us from distant sources would be deflected by intermediate matter. This so called gravitational lensing phenomena provides us a unique tool to map the distribution of matter in our universe and constrain parameters in our cosmological models. To understand the basic key concepts of gravitational lensing theory (such as deflection angle, lens equation, critical curves and caustics) you can learn them from the lab of strong gravitational lensing or read yourself the review by Narayan & Bartelmann (1996). In this manual, we will focus on the theory and observables that are more relevant to the weak gravitational lensing regime. One can refer to Schneider et al. 2006 and Halder et al. 2021 for more details discussed in this section.

4.1 Weak lensing basics

In weak gravitational lensing, emitted light from the source object will be deflected by the intervening matter. The deformation of a lensed image with respect to its unlensed image can be represented by a distortion matrix $\mathcal{A}$:

$$\mathcal{A} = \frac{\partial\left(\delta\vec{\beta}\right)}{\partial\left(\delta\vec{\theta}\right)} = \begin{pmatrix} 1-\kappa-\gamma_1 & -\gamma_2 \\ -\gamma_2 & 1-\kappa+\gamma_1 \end{pmatrix} \tag{45}$$

$$= (1-\kappa)\begin{pmatrix} 1 & 0 \\ 0 & 1 \end{pmatrix} - \gamma\begin{pmatrix} \cos(2\phi) & \sin(2\phi) \\ \sin(2\phi) & -\cos(2\phi) \end{pmatrix}, \tag{46}$$

where $\delta\vec{\beta}$ and $\delta\vec{\theta}$ are differential angular position vectors of source and images respectively as denoted in Figure.1. Here we have also introduced several new quantities: κ is the convergence and γ is the modulus of the shear $\gamma = \sqrt{\gamma_1^2 + \gamma_2^2}$. Shear itself is a complex vector $\vec{\gamma} = \gamma_1 + i\gamma_2 = \gamma e^{2i\phi}$ and ϕ is the orientation angle of the shear.

The effects of distortion represented by equation (46) can be understood schematically from Figure 2 in which we show how the gravitational lensing distorts the image of a source galaxy whose projected shape in the sky is assumed to be intrinsically circular. From the equation we see that convergence is only attached to an identity matrix, indicating that convergence would not add correlation to the two components of the angular position vector of the source galaxy and it is only responsible for magnifying the source image isotropically. Moreover, we have $\kappa < 1$ for the weak gravitational lensing. On the other hand, shear is expressed with a rotation-like matrix, implying that it would rotate and stretch the source image, i.e. introducing anisotropy into the shape of a galaxy image. Unlike strong gravitational lensing, weak lensing cannot produce multiple images but only the above distortion effects on the single image. Such a schematic illustration can be seen in Figure.3.

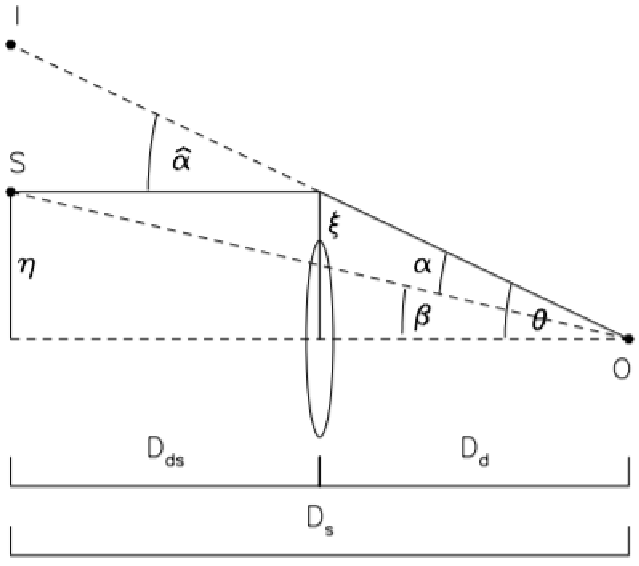

Figure 1: Illustration of a lensing system. Point "S", "I" and "O" denote for source, deflected image and observer respectively. At the bottom are distances between source, lens and the observer. Light emitted by a source which has a distance η from the central optical axis and propagates parallel to it is deflected by an angle $\hat{\alpha}$ and then reaches the observer. The resulting image would have an angular separation θ from the optical axis in the sky which is different from the actual separation of the source β. Image from Narayan & Bartelmann (1996).

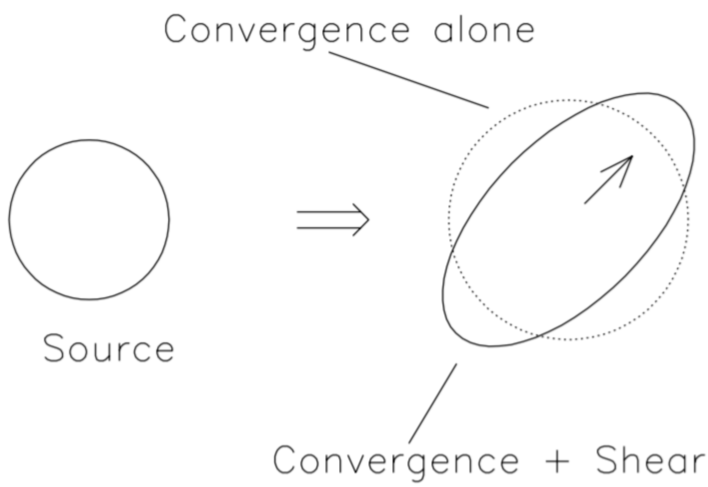

Figure 2: Effects of lensing distortion. For an intrinsically circular source galaxy, convergence will magnify its size isotropically and shear will turn it into an ellipse and thus introduce anisotropy in its shape. Image from Narayan & Bartelmann (1996).

4.2 Weak lensing measurement

4.2.1 Shear estimation

In weak lensing regime, a source object is usually a distant galaxy whose image is distorted by the foreground matter. What we can observe directly through photometric surveys such as Dark Energy Survey (DES) is the shape of each galaxy, characterised by its ellipticity. It is the shear field that induces ellipticities (i.e. results of the image distortion) as mentioned in the previous

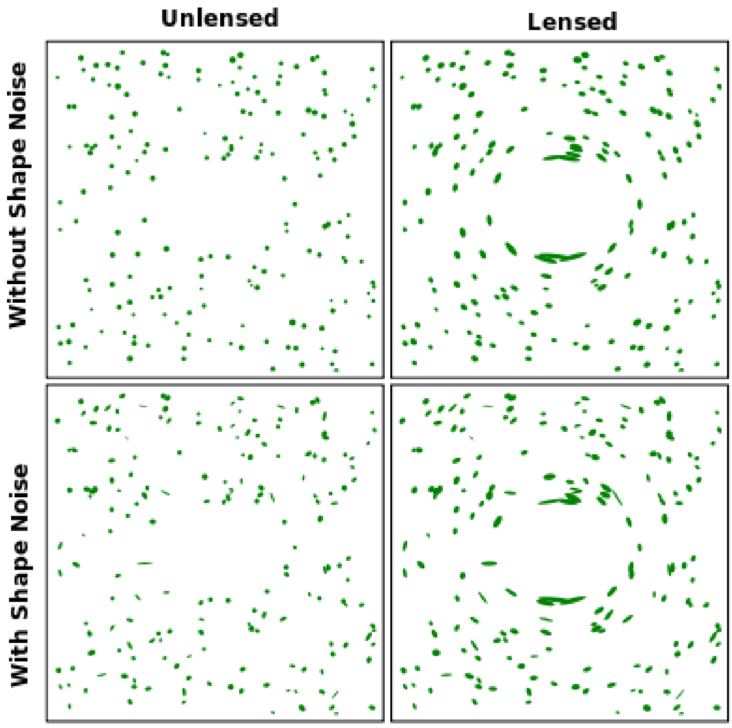

Figure 3: Effects of weak gravitational lensing distortion. One can take every green dot as a source galaxy. No multiple images are produced from each unlensed source. In the above panel, every source galaxy is assumed to be circular for its projected shape in the sky. In the bottom panel, each source galaxy has its own intrinsic ellipticity before being weakly lensed. Image from https://en.wikipedia.org/wiki/Weak_gravitational_lensing.

section and there are many approaches to infer the shear field from those measured ellipticities assuming that the intrinsic galaxy shapes are on average circular.

The first question we need to address is what is the origin of the shear field? Since it is gravity that deflects the light and distorts the images, the answer is not hard to guess. The shear field must be induced by the mass concentration between the source and the observer.

Just as the gravitational field can be expressed as the derivative of the gravitational potential, the shear field can also be written as the derivative of a corresponding lensing potential from large scale structures (Kilbinger, 2015):

$$\Psi(\vec{\theta},\chi) = \frac{2}{c^2}\int_0^{\chi} \mathrm{d}\chi' \frac{f_k(\chi-\chi')}{f_k(\chi)f_k(\chi')}\Phi(f_k(\chi')\vec{\theta},\chi')\,, \tag{47}$$

where χ is the radial comoving distance and $f_k(\chi)$ is the comoving angular diameter distance in a space with curvature k which would be equal to χ if the universe is flat. Φ is the Newtonian gravitational potential and here the lensing potential at a point in space is a weighted sum of the Newtonian potential between the observer and that point. c is the speed of light and $\vec{\theta}$ is the two-dimensional angular position vector in the sky.

The shear field comes from the second order derivative of the lensing potential with respect to the angular coordinates:

$$\gamma_1 = \frac{1}{2}(\Psi_{,11} - \Psi_{,22}) \tag{48}$$

$$\gamma_2 = \Psi_{,12} \ , \tag{49}$$

where $\Psi_{,ij} = \partial\Psi/(\partial\theta_i\partial\theta_j)$. Here the two components of the shear $\gamma_1(\vec{\theta})$ and $\gamma_2(\vec{\theta})$ are specified in a chosen Cartesian coordinate at a given location $\vec{\theta}$ with respect to a reference point in a 2D flat sky. However, we can also decompose the shear field into two components defined with respect to the angular position[5] $\vec{\theta}$: the tangential shear γ_t and cross shear $\gamma_\times$. Their relations to the γ_1 and γ_2 are:

$$\gamma_t = -\gamma_1 \cos 2\vartheta - \gamma_2 \sin 2\vartheta \tag{50}$$

$$\gamma_\times = -\gamma_1 \sin 2\vartheta + \gamma_2 \cos 2\vartheta \ . \tag{51}$$

A clear explanation can be seen in Figure 4. Suppose the matter distribution between the

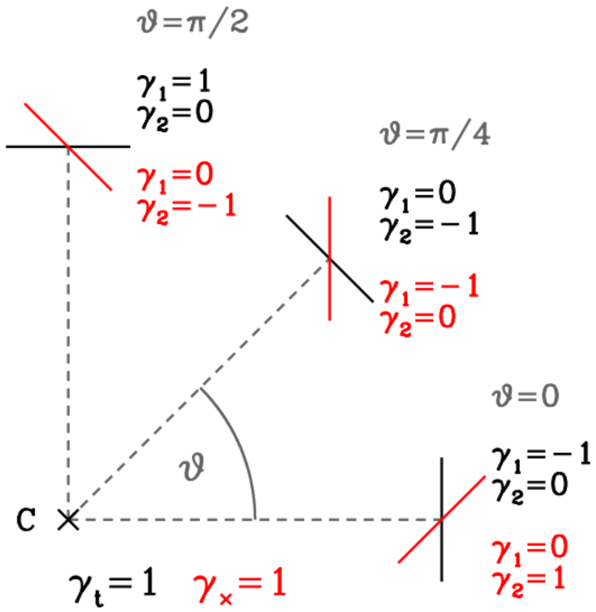

Figure 4: C is the central reference point. Tangential shear γ_t is defined perpendicular to or along the line connecting the field and the reference point. Cross shear $\gamma_\times$ is defined with the directions of tangential shear rotating 45°. In this figure, the direction perpendicular to the radial direction is defined as the positive axis for the tangential shear and after rotating it 45° clockwise the positive axis for cross shear is defined. Therefore at three different angular positions, the tangential and cross shear which are represented by the black and red bars are of constants. However, the values of corresponding γ_1 and γ_2 are different following the inverse transformations shown in equation (50) and equation (51). Image adopted from Gruen 2015.

source and the observer has spherical symmetry, then the weak lensing distortion should perfectly place the lensed galaxy images along the tangential direction with respect to the center of mass concentration and the cross shear will always be zero. Another issue to notice is that

[5] In 2D polar coordinates, the angular posotion $\vec{\theta}$ can be decomposed into a radial length θ and a polar angle ϑ with respect to a reference point.

the same value of tangential and cross shear correspond to different values of γ_1 and γ_2 for field points at different angular positions in the sky.

Aside from the induced ellipticity by the shear field, the unlensed galaxy image would have an intrinsic ellipticity from its original shape projected in the sky (also referred to as shape noise in Fig.3). Assuming there are no additional distortion from observational systematic errors, the relation between the observed ellipticity $e^{\rm obs}$ and the intrinsic ellipticity $e^{\rm int}$ of a galaxy is:

$$e^{\rm obs} = \frac{e^{\rm int} + \gamma}{1 + \gamma^* e^{\rm int}} , \tag{52}$$

where γ^* represents the complex conjugate of the shear field but not the modulus of the shear as denoted in the previous section. The ellipticity itself depends on how observations measure the light distribution of a galaxy and there can be various definitions (Schneider et al. 2006). It is infeasible in weak lensing regime to probe the shear value at a point in the field by measuring the ellipticity of just one neighboring galaxy since both observed and intrinsic ellipticities are hard to measure and the results would be highly inaccurate. However, based on one **critical assumption** that unlensed galaxies are oriented randomly (Schneider et al. 2006), if we measure sufficiently large number of galaxies around that field point and take the ensemble average of the observed ellipticities, the ensemble average of intrinsic ellipticities would vanish due to their random orientations and we are left with $\langle e^{\rm obs} \rangle \approx \gamma$. This is only an approximation and what scientists actually measure from ellipticities is a quantity called reduced shear:

$$g = \frac{\gamma}{1 - \kappa} , \tag{53}$$

which in the limit of weak lensing regime would become $g \approx \gamma$ since $\kappa \ll 1$. In our lab, we will consider $e^{\rm int} = 0$ and thus $e^{\rm obs} = \gamma$.

Exercise:

- **T3**: Following the tangential and cross shear convention in Figure.4, we assume that $\gamma_1 = 0.3$ and $\gamma_2 = 0.0$ for all $\theta = 0^\circ, 45^\circ$ and 90°. Please compute the corresponding $\gamma_{\rm t}$ and $\gamma_\times$ at all three different angular positions. Also explain the positive and negative signs in front of each $\gamma_{\rm t}$ and $\gamma_\times$.

4.2.2 Convergence and its relation to the shear

Lensing convergence κ is another quantity that has been introduced in the previous section. Like the shear field, the convergence field can be derived from the second order derivative of the lensing potential as well:

$$\kappa = \frac{1}{2} \nabla_\theta^2 \Psi , \tag{54}$$

where ∇_θ^2 is a two-dimensional Laplacian operator with respect to the angular coordinates. We can substitute the lensing potential in equation (47) with the expression in equation (54) and notice that since the Laplacian operator acts on angular coordinates, it can only operate with the Newtonian potential within the integrand. By introducing the Poisson equation in comoving coordinates, we are able to write the convergence at a given point in space as:

$$\kappa(\vec{\theta}, \chi) = \frac{3 H_0^2 \Omega_m}{2c^2} \int_0^\chi {\rm d}\chi' \frac{f_k(\chi - \chi') f_k(\chi')}{f_k(\chi)} \frac{\delta_m(f_k(\chi')\vec{\theta}, \chi')}{a(\chi')} , \tag{55}$$

where H_0 is the Hubble parameter at redshift zero, Ω_m is the density parameter of total matter in the universe. $\delta_m(f_k(\chi)\vec{\theta},\chi)$ is the matter density perturbation field following the definition in equation (22) and $a(\chi)$ is the scale factor. There is a nice interpretation of the equation above which can be understood as follows. If a single light source is located at comoving distance χ with angular position $\vec{\theta}$, then the lensing convergence that a light ray bundle from the source experiences on its way towards the observer is given by a weighted sum of the contributions from all the matter density distribution between the observer and the source.

We can further assume that multiple source objects follow a (normalised) redshift distribution $p_s(z)$ along the line-of-sight with the corresponding distribution in comoving distance being $n_s(\chi)$ i.e. $n_s(\chi)\mathrm{d}\chi = p(z)\mathrm{d}z$. In this case, the mean convergence towards direction $\vec{\theta}$ becomes:

$$\kappa_{\mathrm{eff}}(\vec{\theta}) = \int_0^{\chi_{max}} \mathrm{d}\chi\, n_s(\chi)\kappa(\vec{\theta},\chi) \tag{56}$$

$$= \frac{3H_0^2\Omega_m}{2c^2}\int_0^{\chi_{max}} \mathrm{d}\chi\, g(\chi) f_k(\chi)\frac{\delta_m(f_k(\chi)\vec{\theta},\chi)}{a(\chi)}\,, \tag{57}$$

where χ_{max} is the maximal radial comoving distance (e.g. the horizon of the observable universe) and $g(\chi)$ reads:

$$g(\chi) = \int_\chi^{\chi_{max}} \mathrm{d}\chi' n_s(\chi')\frac{f_k(\chi'-\chi)}{f_k(\chi')}\,. \tag{58}$$

From the above discussion, we know that both shear and convergence are derived from the second order derivative of the lensing potential. Therefore, it is clear that shear and convergence are not independent from each other. It is easier to write down their relation in Fourier space where the 2D angular position $\vec{\theta}$ transforms to the multipole $\vec{\ell}$:

$$\gamma(\vec{\ell}) = \frac{(\ell_x + \mathrm{i}\ell_y)^2}{\ell^2}\kappa(\vec{\ell}) = e^{2\mathrm{i}\phi_\ell}\kappa(\vec{\ell})\,, \qquad \ell \neq 0 \tag{59}$$

where $\ell = \sqrt{\ell_x^2 + \ell_y^2}$ and $\phi_\ell = \arctan(\frac{\ell_y}{\ell_x})$ is the polar angle of $\vec{\ell}$.

Exercise:
• **T.Optional**: Show the derivation which allows you to explicitly write down the integral expression of $g(\chi)$ in equation (58). In equation (56) discuss the reason for the integration limits of $\kappa_{\mathrm{eff}}(\vec{\theta})$ i.e. the inner integration over χ' and the outer integration over χ. **Hint**: When starting from equation (56), try to apply Fubini's theorem[6] to the double integral. You can use the flat universe assumption for terms involving $f_k(\chi)$ to ease your derivation.

5 Weak gravitational lensing statistics

In this section, we are going to combine what we have introduced in the previous two sections and build 2-point statistical models for weak gravitational lensing observables, in this case weak lensing shear specifically. Later on students will compare the theoretically computed 2PCF of shear to that measured from N-body simulations and therefore validate the modelling.

[6] A simple illustration can be seen in this webpage: https://mathinsight.org/double_integral_examples

5.1 Shear 2PCF and its relation to the convergence 2PCF

By definition (Schneider and Lombardi, 2003), the 2PCF of shear has two branches: one is the plus shear 2PCF, ξ_+ and the other is the minus shear 2PCF, ξ_-[7]. Students should now recall our previous discussion about tangential and cross shear components as we will use them to define the shear 2PCFs.

Suppose we have two points in the sky with respective 2D angular positions $\vec{\theta_1}$ and $\vec{\theta_2}$ and these two points are separated by a separation vector $\vec{\alpha}$. We can write down the tangential and cross shear at each of these two positions as $\gamma_{t,1}$, $\gamma_{t,2}$ and $\gamma_{\times,1}$, $\gamma_{\times,2}$. Then the shear 2PCFs are defined as:

$$\xi_+(\vec{\alpha}) \equiv \langle\gamma_{t,1}\gamma_{t,2}\rangle + \langle\gamma_{\times,1}\gamma_{\times,2}\rangle = \langle\gamma(\vec{\theta_1})\gamma^*(\vec{\theta_2})\rangle \tag{60}$$

$$\xi_-(\vec{\alpha}) \equiv \langle\gamma_{t,1}\gamma_{t,2}\rangle - \langle\gamma_{\times,1}\gamma_{\times,2}\rangle = \langle\gamma(\vec{\theta_1})\gamma^*(\vec{\theta_2})e^{-4i\phi_\alpha}\rangle\ , \tag{61}$$

where γ is the complex shear introduced in section 3.1 and ϕ_α is the polar coordinate of the separation vector $\vec{\alpha}$. From the discussion in section 2.2, we know that equation (60) and equation (61) can be rewritten as the 2D inverse Fourier transform of the corresponding power spectrum. Now if we apply the relation between Fourier space 2D shear and convergence in equation (59) to the definition of power spectrum in equation (32), we can obtain the relation between 2D power spectrum of shear and convergence:

$$P^{2D}_\gamma(\vec{\ell}) = \langle\gamma^*(\vec{\ell})\gamma(\vec{\ell})\rangle = \langle e^{-2i\phi_\ell}\kappa^*(\vec{\ell})e^{2i\phi_\ell}\kappa(\vec{\ell})\rangle = P^{2D}_\kappa(\vec{\ell})\ . \tag{62}$$

Based on equation (62), we can now express the shear 2PCFs in terms of convergence power spectrum. Though one thing to notice here is that in ξ_- we have this extra phase factor and its counterpart in Fourier space would be $e^{-4i\phi_\ell}$. In conclusion, the shear 2PCFs can be written down as:

$$\xi_+(\alpha) = \mathcal{F}^{-1}[P^{2D}_\kappa(\ell)] = \int \frac{\mathrm{d}\ell\ell}{2\pi} P^{2D}_\kappa(\ell)J_0(\ell\alpha) \tag{63}$$

$$\xi_-(\alpha) = \mathcal{F}^{-1}[P^{2D}_\kappa(\ell)e^{-4i\phi_\ell}] = \int \frac{\mathrm{d}\ell\ell}{2\pi} P^{2D}_\kappa(\ell)J_4(\ell\alpha)\ , \tag{64}$$

where in the above two equations we again exploit the isotropic property of density field statistical measurement and do not consider the direction of the separation vector but only its modulus. equation (63) essentially is the 2D version of equation (34) when we only consider the real value component in it. equation (64) has a similar form but different weighting for multipoles due to the extra phase factor. J_0 and J_4 are the zeroth and fourth-order Bessel functions of the first kind respectively. These equations are known as Hankel transforms[8]. **An important remark** here is that for our lab we will not evaluate the above Hankel transforms as written in the equations above. Instead, we will replace the integration in equations (63) and equation (64) with similar kind of summations introduced in equation (41) involving associated Legendre polynomials. These summations are efficient and numerically stable ways to evaluate the Hankel transforms above and the relevant code to perform them will be provided in the lab

[7] To be precise, there is also the cross plus and minus correlations but they will vanish when the shear field is statistically invariant under parity transformations

[8] Hankel transforms express any given function as a weighted sum of an infinite number of Bessel functions of the first kind. They are also known as Fourier-Bessel transforms.

exercise folder (explaining the exact expressions for these summations are beyond the scope of this manual but the interested student can look them up in the provided code and the references therein).

So much for the theory, in practice, one actually estimates the shear 2PCFs in equations (60) and (61) from the observed ellipticities of galaxies (note that in the lab we assume $e^{\rm obs} = \gamma$) and they are measured as follows (Troxel et al. 2018):

$$\hat{\xi}_{\pm}(\alpha) = \frac{\sum_{i,j} w_i w_j (\gamma_{\rm t}^i \gamma_{\rm t}^j \pm \gamma_{\times}^i \gamma_{\times}^j)}{\sum_{i,j} w_i w_j} \tag{65}$$

where i, j are the indices of a pair of observed galaxies which are separated by an angular separation α. The w_i are the weights associated to each observed galaxy (in our lab $w_i = 1$). For our exercises we will use the publicly available software `TreeCorr` (see Section 5.3) which has a fast implementation of equation (65) for computing the $\xi_{\pm}$ from data.

5.2 2D power spectrum of convergence

Coming back to our theoretical modelling, the final step before we can have a complete analytical model for the shear 2PCFs is to express the 2D convergence power spectrum explicitly. From equation (57), we see clearly that convergence is a weighted line-of-sight projection of matter density perturbation. If we combine this understanding with the projection of 3D power spectrum in equation (43), it's straightforward for us to say that the 2D convergence power spectrum P_{κ}^{2D} is a weighted line-of-sight projection of the 3D matter power spectrum $P_{\delta_m}^{3D}$.

The weighting kernel q in equation (43) for lensing is (we call this the lensing kernel):

$$q(\chi) = \frac{3H_0^2\Omega_m}{2c^2} g(\chi) \frac{f_k(\chi)}{a(\chi)} , \tag{66}$$

where $g(\chi)$ and $f_k(\chi)$ are the same as in equation (57). Previously in the **Optional Exercise** we have derived the formula for $g(\chi)$ which students should now realise that it contains weak lensing source distribution $n_s(\chi)$. In this lab, we shall assume that the source redshift distribution is a Dirac delta function $\delta_D(\chi - \chi_s)$, implying that all weak lensing sources are located at the same redshift corresponding to the comoving distance χ_s. Then for the 2D convergence power spectrum where we have the case that $q_1(\chi)$ and $q_2(\chi)$ in equation (43) are identical, we have the following expression:

$$P_{\kappa}^{2D}(\ell) = \frac{9H_0^4\Omega_m^2}{4c^4} \int_0^{\chi_s} {\rm d}\chi \left(\frac{\chi_s - \chi}{\chi_s\, a(\chi)}\right)^2 P_{\delta_m}^{3D}\left(|\vec{k}| = \frac{|\vec{\ell}|}{\chi}, \chi\right). \tag{67}$$

By changing the variable as ${\rm d}\chi = c{\rm d}z/H(z)$, equation (67) can be written as an integration in redshift space:

$$P_{\kappa}^{2D}(\ell) = \frac{9H_0^4\Omega_m^2}{4c^4} \int_0^{z_s} \frac{c{\rm d}z}{H(z)} \left(\frac{\chi_s - \chi(z)}{\chi_s}(1+z)\right)^2 P_{\delta_m}^{3D}\left(|\vec{k}| = \frac{|\vec{\ell}|}{\chi(z)}, z\right). \tag{68}$$

Exercise:

• **T4**: For a Dirac delta source redshift distribution $n_s(\chi)$, write down the explicit formula for $g(\chi)$ in equation (58) and the corresponding lensing kernel $q(\chi)$ in equation (66). Then based on equation (43), equation (57) and equation (66), derive equation (67).

5.3 Matter power spectrum

Now students may ask: But we still don't know how to quantify the 3D matter power spectrum $P^{3D}_{\delta_m}(k,z) \equiv P_{\delta_m}(k,z)$ and without this knowledge how can we obtain the final model for P^{2D}_{κ} and eventually the shear 2PCFs $\xi_{\pm}$?

Indeed, finding a correct way to describe the matter power spectrum in our Universe is not a simple task. In this manual, we will only provide a brief discussion that is relevant to the lab content. Students who are interested can find more details in the institute's cosmology lectures or textbooks such as Dodelson & Schmidt, 2020. **Students are not required to write down matter power spectrum analytically and do the relevant coding work themselves**. This subsection is mainly for a theoretical understanding purpose.

The cosmological analysis of the initial conditions in our Universe shows that the primordial dimensionless matter power spectrum is almost scale-invariant:

$$\Delta_i^2(k) = \frac{k^3 P^i_{\delta_m}(k)}{2\pi^2} \propto k^{n_s - 1} , \tag{69}$$

where the scalar spectral index n_s is constrained to be 0.9649 ± 0.0042 at 68% confidence level according to the Planck results. One important cosmological parameter to introduce here is A_s which characterises the amplitude of this primordial matter power spectrum. After the primordial phase, our Universe consecutively enters epochs in which the dominant energy component is radiation and matter respectively. During these epochs, the shape of the dimensionless matter power spectrum will be changed due to the structure growth. And this shape change can be described in terms of the transfer function $T(k)$ which transfers the initial dimensionless power spectrum of comoving curvature perturbations $\Delta^2_R \propto \Delta^2_i(k)$ to its value today:

$$\Delta^2(k, a=1) \propto k^4 T(k)^2 k^{n_s - 1} , \tag{70}$$

where the transfer function will be computed numerically by a code package in this lab.

If we also consider the component of dark energy and only keep the linear term of density perturbation when we solve the evolution equations, the growing solution for the matter is:

$$\delta_m(\vec{x}, t) = D(t)\delta_m(\vec{x}) , \tag{71}$$

where D is called the growth factor and from the above equation one can observe that the time and spatial evolution of matter density in the linear perturbation regime is independent from each other. In the late time Universe, A_s can be reparametrized as σ_8 which describes the variance of the matter density fluctuations in spheres of radius 8 Mpc/h. This parameter will be used in later practical exercises.

Exercise:

• **T5**: Based on the simplified discussion on the linear perturbation, try to find the dependence of linear matter power spectrum $P^{lin}_{\delta_m}(k,z)$ on the wavenumber k, the transfer function $T(k)$ and the growth factor $D(t)$ (or $D(z)$). Write it down in a proportionality relation.

However, the above linear theory only works in the regime where the matter density perturbation is very small $\delta_m \ll 1$. In order to describe the real matter power spectrum in the Universe, linear regime is not accurate enough. We have to solve for the matter power spectrum in the non-linear regime where $\delta_m \gg 1$. To do that, two major approaches are available: One is to solve the differential evolution equations in the context of higher-order, nonlinear perturbation theory. The other is to run N-body simulations which capture the realistic gravitational interactions and invent a fitting formula with many free parameters to be optimised for the matter power spectrum and calibrate the fitting formula against the corresponding measurements from simulations. In this lab, we are going to use a fitting formula from the second approach called "Halofit" (Takahashi et al. 2012) to calculate the matter power spectrum for different cosmological parameters. We will use CLASS to compute the matter power spectrum, please refer to Section 5 for information regarding it.

Exercise:
• **T6**: In the lab we will work with the publicly available N-body simulation data set of Takahashi et al., 2017 (or T17 simulation to be simple). Therefore, we need to find the corresponding cosmological parameters of that simulation suite for which we would need to compute various cosmological terms such as the matter power spectrum, Hubble parameter etc. Open the relevant paper (https://arxiv.org/pdf/1706.01472.pdf) and find the cosmological parameters of the T17 simulation. You should tabulate these values in your report and mention from which Section of the paper you obtained them.

6 Software tools to be used in this lab

6.1 CLASS

CLASS — the Cosmic Linear Anisotropy Solving System (Lesgourgues et al. 2011) — is a code package written in an object-oriented style with an available python wrapper[9]. It can be used to simulate many important CMB (Cosmic Microwave Background) and large scale structure observables. In this lab, we will use CLASS to compute the nonlinear matter power spectrum $P_{\delta_m}(k, z)$ which is a critical component in our modelling for the shear 2PCFs as discussed in previous sections.

A simple way to understand CLASS in this lab is to think of it as a machinery that takes in an input dictionary which contains cosmological parameters, the desired target output and relevant free parameters. The code package will then solve a system of evolution equations, including the transfer function mentioned above, based on the cosmological information provided by the input dictionary and return a python class object [10]. One can call many functions (methods) from this python class object to compute the specified target output and other background quantities. These can be the matter power spectrum, Hubble parameter, angular diameter distance and so on. Since many such quantities evolve along with the redshift z, one needs to give the corresponding value to those functions for them to calculate. Below we will show an illustration example about CLASS that can better enable students to work with it.

[9] https://lesgourg.github.io/class_public/class.html
[10] For students who are not familiar with the concept of class in python, this link: https://www.w3schools.com/python/python_classes.asp provides a quite clear explanation.

6.1.1 An example of CLASS

```
import numpy as np
from classy import Class

# Set up the input parameters #
Omega_m = 0.3    # matter density parameter
Omega_b = 0.043    # baryon density parameter
h = 0.7    # reduced Hubble parameter H/100
n_s = 0.96    # scalar spectral index
sigma8 = 0.81    # characterisation of power spectrum amplitude
nonlinear_model = "Halofit"    # nonlinear modelling recipe
kmax_pk = 50.0
z_max_pk = 2.5

# Write down the input dictionary #
commonsettings = {
'N_ur' :3.046,
'N_ncdm' :0,
'output' :'mPk',
'P_k_max_1/Mpc' :kmax_pk,
'omega_b' :Omega_b * h**2,
'h' :h,
'n_s' :n_s,
'sigma8' :sigma8,
'omega_cdm' :(Omega_m - Omega_b) * h**2,
'Omega_k' :0.0,
'Omega_fld' :0.0,
'Omega_scf' :0.0,
'YHe' :0.24,
'z_max_pk' :z_max_pk,
'non linear' :nonlinear_model,
'write warnings' :'yes' }

# Set up the CLASS object and compute it #
Cosmo = Class()
Cosmo.set(commonsettings)
Cosmo.compute()

# several functions on can call from python class object Cosmo #
print(Cosmo.Hubble(0.5))
print(Cosmo.angular_distance(1.0))
print(Cosmo.pk(1.0, 0.2))
```

There are several things to pay attention in the above example code:

1. **from classy import Class** is the line which imports the python wrapper of the CLASS code package. CLASS will be installed beforehand and students should be able to import it.

2. In the input dictionary, we give 'mPk' to the key 'output' since this tells CLASS that we want the matter power spectrum as the target output. Another two keys 'P_k_max_1/Mpc' and 'z_max_pk' fix the maximum wavenumber and redshift for the matter power spectrum computation.

3. For density parameter keys in the dictionary, names starting with lower case letter is the physical density parameter and is equal to the density parameter multiplied by h^2 (e.g. $\omega_b = \Omega_b \times h^2$). Also in CLASS, one cannot directly input the total matter density parameter. Instead it can be decomposed into cold dark matter, baryon and non-cold dark matter particles such as neutrinos (e.g. $\Omega_m = \Omega_{cdm} + \Omega_b + \Omega_\nu$).

4. In the above code, we assume a flat universe and set the curvature density parameter 'Omega_k' to be zero. And when considering the dark energy, we assume the ΛCDM model with cosmological constant. That's why we do not adopt the dynamic equation of state ('Omega_fld' = 0.0) or the scalar field model ('Omega_scf' = 0.0). From all the other energy components, CLASS will automatically infer the density parameter of dark energy.

5. In the last three lines, we ask the CLASS object to compute three different quantities: Hubble parameter, angular diameter distance and matter power spectrum. The first two are functions of redshift. The last one is a function of (k, z). All wavenumbers in the above code have the unit of Mpc^{-1}.

6. As we introduced in section 4.3, one can use fitting formula calibrated from N-body simulations to describe the nonlinear matter power spectrum. Here we use the specific "Halofit" which is also what we shall use through the whole lab. However, there are other options for nonlinear fitting (e.g. HMcode) which have their own features.

Exercises:
- **P1.1**
- **P1.2**
- **P1.3**
- **P1.4**
- **P1.5**
- **P1.6**

All the practical exercises are collected in Section 6.

6.2 Healpy - working with random fields on the sphere

As mentioned in the previous sections, for the purpose of this lab we want to investigate the weak lensing field on the projected 2D sky i.e. on the celestial sphere. In order to achieve this, we use `Healpy`[11] — a Python package which allows one to analyse and visualise data in pixelated format (at a given resolution) on the unit sphere (all-sky).

`Healpy` is a Python wrapper for the Hierarchical Equal Area isoLatitude Pixelisation — HEALPix[12]

[11] currently hosted at https://github.com/healpy/healpy
[12] currently hosted at https://healpix.sourceforge.io/

C++ library (Zonca et al. 2019). The pixelisation is a process to subdivide the spherical surface of the sphere into many pixels such that every pixel covers the same surface area. Each pixel on the sphere can be characterised by two angular coordinates written together as the direction vector $\hat{r}$ (see section 3.2.2). We shall refer to the size of a single pixel as the 'pixel scale'. The area of a pixel depends on the resolution of the map which can be set using the `healpy` keyword[13] `NSIDE`. This keyword defines the total number of pixels N_{pixel} which make up the full sky map:

$$N_{pixel} = 12 \cdot \texttt{NSIDE}^2 \, . \tag{72}$$

As an example, if the resolution of a `healpy` sky-map was kept at `NSIDE` = 1024, implying that $N_{pixel} = 12582912$ (from equation (72)). This results in a pixel area of $A_{pixel} = 3.3 \cdot 10^{-3}$ square degree (computed using `healpy`'s `nside2pixarea` routine). The pixel smoothing scale can roughly be estimated by:

$$\theta_{pixel} \approx \sqrt{A_{pixel}} \tag{73}$$

which gives a scale of $\theta_{pixel} \approx 3.43$ arcmins.

Higher resolutions i.e. larger values of `NSIDE` result in a higher number of pixels covering the full surface of the sphere. This leads to a smaller area A_{pixel} for each pixel or in other words a smaller pixel smoothing scale θ_{pixel}. One should note here that due to the internal functionality of `healpy`, `NSIDE` is required to have a value which is a power of 2.

Exercise:
- **P2.1**
- **P2.2**
- **P2.3**

All the practical exercises are collected in Section 6.

6.3 TreeCorr - computing angular correlation functions

In equation (65) we saw how one can estimate the shear 2PCF from observed galaxy ellipticities. This estimation of the shear 2PCF from data actually involves finding all possible pairs of points on the random field located at $\hat{r}^i$ and $\hat{r}^j$ which are separated by an angular separation α i.e. $\hat{r}^i \cdot \hat{r}^j = \cos\alpha$ and then computing the average of the product of the shear values evaluated at those points as shown already in equations (60) and (61).

However, when we want to perform this on data on the sphere, it should be noted that effects such as the resolution of the data (e.g. for `healpy` images, the pixel size A_{pixel}) does not allow one to distinguish points ($\hat{\mathbf{n}}$) which are separated below this limiting size (pixel scale). Hence, this aspect has to be taken into account while computing pairs of points on data. Moreover, finding all possible pairs of points (pixels) is computationally expensive as the pair finding complexity scales as $\mathcal{O}(N_{pixel}^2)$.

There are a number of algorithms which can compute correlations from flat 2D image data. However, for our lab as we want to compute correlations from data defined on the 2D sphere,

[13] you should read more about the different Healpy keywords and routines used in this lab from the online documentation hosted at https://healpy.readthedocs.io/en/latest/index.html

we use a publicly available numerical code called `TreeCorr`[14] (Jarvis et al. 2004) which is a software for efficiently computing 2 and 3-point correlation functions of a given field (scalar or vector) such as density contrast, number counts, weak lensing shear field, CMB temperature fluctuations etc. Using parallel computing, it can compute the correlations of fields defined in both 3D Euclidean space or in the curved 2D sky (in Right Ascension (RA) and declination (dec) coordinates of the sky-map's pixels) efficiently using the so called 'ball-tree' algorithm. Hence, we use `TreeCorr` for computing the angular shear 2PCF $\xi_{\pm}(\alpha)$ of a weak lensing shear field γ on the celestial sphere:

$$\boxed{\gamma \rightarrow TREECORR \rightarrow \xi_{\pm}(\alpha)}$$

This is achieved by using the `GGCorrelation`[15] method from `TreeCorr`.

Exercise:
- **P2.4**
- **P2.5**
- **P2.6**
- **P2.7**

All the practical exercises are collected in Section 7.

[14] currently hosted at https://github.com/rmjarvis/TreeCorr
[15] see https://rmjarvis.github.io/TreeCorr/_build/html/gg.html

7 The lab

First day of lab

• **P1.1**: Use the example code in section 6.1.1 (already provided in the accompanying jupyter notebook) to perform the following:

(i) Run the code in your machine and see if you can have three values printed out. They should be the three quantities CLASS is asked to compute at the end of the code.

(ii) Now plot the Hubble parameter[16] $H(z)$ and angular diameter distance $d_A(z)$ as functions of redshift z. Also plot the corresponding comoving distance $\chi(z)$ using equation (21) and compare it to the $d_A(z)$. The redshift z range can be set to a linear scale that is evenly spaced from 0.0 to 2.0 with 100 intervals (you can use `np.linspace`)

(iii) Then fixing the redshift at 0.0, 1.0 and 2.0 try to plot the matter power spectrum as a function of wavenumber k for all the three redshifts. The wavenumber k range can be set to a logarithmic scale from 0.001 Mpc^{-1} to 30 Mpc^{-1} with 100 bins (you can use `np.logspace`).

In most of the following exercises, you can use the same arrays of redshift z and of wavenumbers k that you have created here.

• **P1.2**: In the lab (on the second day), we will measure the shear 2PCFs from the publicly available simulation data set of Takahashi et al., 2017 (or T17 simulation). Therefore, we need to start working with the T17 cosmological parameters in this and the following exercises.

(i) In exercise **T6** you have already found the cosmological parameters of the T17 simulation. Start a new python script (or a new cell in a jupyter notebook) and compute the same three quantities as you did in **P1.1** (i) but using the cosmological parameters of the T17 simulation.

• **P1.Optional**: With the same example code in section 6.1.1,

(i) Compute and plot the matter power spectrum at redshift $z = 0, 1, 2$ and a sequence of wavenumbers using the T17 cosmological parameters. For convenience use the same wavenumber values as the ones you have used previously. Compare how these spectra differ from those you obtained in exercise **P1.1** (iii).

(ii) After that, switch off the `non linear` parameter (just leave it blank or comment it out) in the example code) such that CLASS would only implement linear perturbation theory in its calculation. Calculate then the matter power spectrum again at the same redshifts and wavenumbers. Plot the linear matter power spectra together with the non linear matter spectra you computed in (i) above and compare their differences, e.g. try to plot the fractional difference, $P_{nl}/P_{lin} - 1$, between the two spectra at the three redshifts. Try to explain the fractional difference between the two spectrum along with the wavenumber k.

[16] Please use the call method "Hubble" from the CLASS object "Cosmo" as in the example code, but just notice that according to CLASS convention, the output of the method is always the real Hubble parameter value divided by the speed of light.

- **P1.3**: In this exercise, you will investigate how cosmological parameters can impact the amplitude and shape of the T17 non linear matter power spectrum at redshift $z = 0.0$. Use the parameter values of T17 simulation that you used in Exercise **P1.2** as reference (fiducial) values.

  (i) If you haven't done the **P1.Optional** exercise above then first compute the non linear matter power spectrum only at redshift $z = 0.0$ for the T17 cosmology at the range of wavenumbers you used in **P1.1** (iii). This will be your 'fiducial' power spectrum.

  (ii) Vary the values of $\Omega_{\rm cdm}$, $\Omega_{\rm b}$, σ_8 and h one by one in turn by 5% (both increment and decrement) with respect to their reference values while keeping others fixed. Plot the fiducial power spectrum and the slightly changed power spectra for a given parameter and observe the differences.

  (iii) Then apply the central difference method[17] to compute the partial derivatives of the matter power spectrum on a range of k with respect to each of these four parameters. Plot these partial derivatives together and try to give a physical interpretation about how the variation of these parameters affect the shape and amplitude of the matter power spectrum.

- **P1.4**: Now recall the concept of weighting or lensing kernel $q(\chi)$ introduced in section 2.2.3 and further elaborated in section 4.2. Suppose that for two cases of line-of-sight projection of the matter power spectrum, the source redshift distributions are Dirac delta functions at $z_{s,1} = 0.5739$ and $z_{s,2} = 1.0344$ respectively.

  (i) Write the two lensing kernels $q(z) \equiv q(\chi(z))$ as python functions of redshift z and compute their numerical values for a series of redshifts between the observer and the source redshift z_s using CLASS. You can decide the redshift spacing up to the source redshift yourself as long as the sampling is dense enough.

  (ii) For each of the two source redshifts $z_{s,1}$ and $z_{s,2}$, plot the corresponding lensing kernels $q(z)$ against redshift z. Discuss at which redshift the matter power spectrum would be weighed the most in equation (43) along the line-of-sight projection for each of the two source redshifts.

- **P1.5**: Based on the equations given in section 4.2, code yourself in python the line-of-sight projection of the matter power spectrum for the two Dirac delta source redshift distributions mentioned in Exercise **P1.4**.

  (i) First you should try to compute the projection at a single multipole number ℓ, say, 1000. **Hint**: Study the expression of the integrand and compute all components as arrays at different redshifts. Then use the trapezoid integration.[18] .

  Note: It is likely that you will run into an error from CLASS (e.g. from the CLASS power spectrum) while performing the line of sight integration: *read the error and try to understand what can be the cause of this*! To solve this you can (i) start the integration in z not exactly from 0 but from a small but finite positive value, and also (ii) change the `kmax_pk` = 50.0 Mpc^{-1} value in your CLASS settings (see the code snippet in Sec 6.1.1)

[17] An explanation of central difference method can be found in:
https://wiki.tum.de/display/modsim/Central+difference+method

[18] For the integration (projection) along the z dimension, you can use numerical methods to solve it such as **np.trapz**: https://numpy.org/doc/stable/reference/generated/numpy.trapz.html

to a higher value e.g. 200 Mpc^{-1}. *Why should these help?* Discuss with your tutor about this.

(ii) Compute the projected 2D convergence power spectrum on a range of multipole numbers. You should start from $\ell = 2$ and end with $\ell = 15000$ with 100 bins in a logarithmic scale, make sure that all bin edges are integer numbers (think how to realise this in python?). Here we ignore the monopole $\ell = 0$ and dipole $\ell = 1$ because when we correct the 2D projected power spectrum to its spherical counterpart according to equation (44) (called the Kitching correction), both the corrected power spectrum values at monopole and dipole will be 0.

(iii) Plot the projected 2D convergence power spectra (after applying the Kitching correction) for both the source redshifts as a function of ℓ.

• **P1.6**: Now that you have the 2D convergence power spectrum at the two source redshifts, input them into the prepared code which very efficiently carries out the computation of the Hankel transforms in equation (63) and equation (64). This will return you the ξ_+ and ξ_- shear 2PCFs at the two different source redshifts on a range of angular separations (5-140 arcminutes in 20 logarithmically spaced angular bins). The exact values of these angular separations are provided in the exercise directory. Plot these shear 2PCFs against the angular bins and save the values into `.txt` or `.dat` files. You will need to compare them to the simulation measurements in the day of the lab.

Second day of lab

Here, we just provide a brief description of the exercises. **You should see the accompanying jupyter notebook for details regarding this part of the lab**.

• **P2.1**: *Working and plotting data on the celestial sphere with* `healpy`. In this exercise you will generate several all-sky `healpy` maps for different NSIDE parameters.

• **P2.2**: *Extracting circular patches on the sphere with* `healpy`. In this exercise you will query circular patches (discs) of radii 2.5 degrees at several locations on an NSIDE=2^{11} `healpy` all-sky map you have created in Exercise **P2.1**.

• **P2.3**: *Importing and checking the simulated weak lensing shear maps from Takahashi simulations (T17)*. In this exercise you will explore the publicly available Takahashi (T17) simulation weak lensing shear (γ_1 and γ_2 components) `healpy` maps at source redshift $z_{s,1}$=0.5739. You will use this data for the next exercises.

• **P2.4**: *Working with TreeCorr: package to compute shear two-point correlation functions (2PCFs)*. In order to measure the shear 2PCFs $\xi_\pm$ from the γ_1 and γ_2 maps at source redshift $z_{s,1}$ you have explored in **P2.3** you will use the publicly available code package `TreeCorr` to compute the 2PCF within a single circular patch of radius 2.5 degrees.

• **P2.5**: *Computing the average shear 2PCFs and their standard deviations in several circular patches in the $z_{s,1}$ map*.

• **P2.6**: *Computing the average shear 2PCFs and their standard deviations in several circular patches in the $z_{s,2}$ map*.

• **P2.7**: *Comparing theory calculations of the shear 2PCFs $\xi_\pm$ against the average of the measurements from the simulations*. Comment on whether your theoretical calculations from **P1.6** agree with your measurements of $\xi_\pm$ or not.

8 Literature

Arfken, G. & Weber, H. 2012, *Mathematical Methods for Physicists: A Comprehensive Guide*, Academic Press.

Bartelmann M., Schneider P., 2001, Phys. Rep., 340, 291

DES Collaboration 2021, arXiv e-prints, p. arXiv:2105.13549

DES Collaboration et al., 2022, PRD, 105, 2

Dodelson, S. & Schmidt, F. 2020, *Modern Cosmology*, Academic Press.

Gott J. et al, 2005, APJ, 624, 463

Gruen, D. 2015, *Weak lensing by galaxy clusters: from pixels to cosmology.*, Dissertation LMU Muenchen: Faculty of Physics.

Halder, A. 2021, MNRAS, 506, 2.

Heymans C., et al., 2021, A&A, 646, A140

Hikage C., et al., 2019, PASJ, 71, 43

Jarvis M., Bernstein G., Jain B., 2004, Monthly Notices of the Royal Astronomical Society, 352, 338

Kaiser, N. 1992, APJ, 388, 272.

Kilbinger, M. 2015, RPP, 78, 8

Kitching T. D., Alsing J., Heavens A. F., Jimenez R., McEwen J. D., Verde L., 2017, Monthly Notices of the Royal Astronomical Society, 469, 2737–2749

LSST Dark Energy Science Collaboration 012, preprint, (arXiv:1211.0310)

Laureijs R., et al., 2011, preprint, (arXiv:1110.3193)

Lesgourgues, J. 2011, arXiv e-prints, arXiv:1104.2932.

Limber D. N., 1954, ApJ, 119, 655

Melchior, P. et al. 2015, MNRAS, 449, 3.

Mukhanov, V. 2005, *Physical Foundations of Cosmology*, Cambridge University Press.

Munoz J. A., Trac H., Loeb A., 2010, MNRAS, 405, 2001

Narayan, R. & Bartelmann, M. 1996, astro-ph/9606001.

Peacock, J.A. 2012, *Cosmological Physics*, Cambridge University Press.

Planck Collaboration. 2020, AAP, 641, A10.

Schneider, P., Kochanek, C.S. & Wambsganss, J. 2006, *Gravitational Lensing: Strong, Weak and Micro*, Springer.

Schneider, P. & Lombardi, M. 2003, AAP, 397, 809.

Spergel D., et al., 2015, arXiv e-prints, p. arXiv:1503.03757

Takahashi, R. et al. 2012, APJ, 761, 2.

Takahashi R., Hamana T., Shirasaki M., Namikawa T., Nishimichi T., Osato K., Shiroyama K., 2017, ApJ, 850, 24

Troxel M., et al., 2018, Physical Review D, 98

Zonca A., Singer L., Lenz D., Reinecke M., Rosset C., Hivon E., Gorski K., 2019, Journal of Open Source Software, 4, 1298